Kinetics of Chiral Symmetry Breaking in Crystallization

Dilip K. Kondepudi,* Kim L. Bullock, Jennifer A. Digits, John K. Hall, and Jason M. Miller

Contribution from the Department of Chemistry, Box 7486, Wake Forest University, Winston-Salem, North Carolina 27109

Received January 25, 1993

Abstract: Results of our study of the kinetics of stirred crystallization that produces large (greater than 99%) asymmetry are presented. The change of concentration with time as the crystallization progresses is obtained for stirred and unstirred crystallizations. A sharp difference in the two concentration vs time curves, due to secondary nucleation in the stirred system, can be observed. Experimental results are compared with the predictions of a set of stochastic kinetic equations. It is found that the proposed kinetics can quite accurately reproduce the experimental data if it is assumed that secondary nuclei are produced in stirred systems only when the parent crystal reaches a minimum size.

Introduction

Nonequilibrium chemical systems can break the symmetries of the underlying chemical reactions. Even though the reaction rate laws of enantiomers are identical, it is possible for a system to produce a large enantiomeric excess.

An example of such chiral symmetry breaking was recently reported for the stirred crystallization of aqueous $NaClO_3$.[1] Though an aqueous solution of $NaClO_3$ is not optically active, the crystals are. Symmetry breaking in this case occurs in a very simple way: if $NaClO_3$ is crystallized from an unstirred solution, statistically equal numbers of levo and dextro crystals are obtained. If the solution is stirred constantly during crystallization, more than 99% of the crystals have the same handedness. In any particular run, the dominance of *l* or *d* crystals is random.

The spontaneous resolution that occurs in this case has some similarities to previous reports,[2,3] but it also has important differences. For chiral symmetry breaking to occur in a chemical system, chiral autocatalysis and competition between enantiomers are generally required. In the case of stirred crystallization, these two processes are realized by the simple act of stirring.

In the context of chiral symmetry breaking, it is interesting to note that at the fundamental level of elementary particles and nuclear reactions, nature is not chirally symmetric.[4,5] For chemical reactions on laboratory time and volume scales, the very small parity violating energy differences between enantiomers due to electroweak interactions between the electron and the nucleons may be disregarded.[6-8]

Symmetry Breaking in $NaClO_3$ Crystallization

The phenomenon of chiral symmetry breaking in $NaClO_3$ crystallization that was reported in an earlier publication[1] is summarized, with additional data, in Figure 1. In this figure the data for percent of *l*-crystals obtained in 60 stirred crystallizations is contrasted with that for 63 unstirred crystallizations (46 from the data of Kipping and Pope[9] and 17 from ours). In the unstirred case, statistically equal numbers of *l*- and *d*-crystals are obtained. The resulting probability distribution for crystal enantiomeric excess is Gaussian-like, as can be seen in Figure 1B. This expected result was demonstrated by Kipping and Pope almost 100 years ago[9] (and repeated by us); it is similar to the result obtained by Pincock et al.[10] for the crystallization of binaphthyl from a melt. Enantiomeric excess obtained from unstirred crystallization is a result of statistical fluctuations, not a process of symmetry breaking as in the case of the stirred crystallization. A large enantiomeric excess can be produced in unstirred crystallization by appropriate seeding. Symmetry breakage through seeding is equivalent to artificially producing a large fluctuation. In the case of $NaClO_3$, it is very easy to produce a large enantiomeric excess by seeding. Kipping and Pope reported[3] that a crystal "... weighing 47 grams, was removed from the solution and broken into small pieces which were seeded into saturated solutions of the chlorate; the latter were then placed aside to crystallize." After a week, it was found that all 269 crystals were dextrorotatory. Other seeding experiments[2] were also found to produce almost 100% *l*- or *d*-crystals if a seed was suspended and the supersaturation was maintained in a specific range. They attributed their results to secondary nuclei produced by dendritic coarsening in which dendrites grow and detach themselves from the suspended seed crystals when the saturation is maintained in a specific range. From these experiments one cannot conclude that in an unseeded crystallization the system is capable of "self seeding" at a supersaturation sufficient to produce very large (99%) asymmetry. In a stirred system such spontaneous production of asymmetry *does* occur due to an interesting interplay between rates of solvent evaporation, secondary nucleation, and crystal growth.

The probability distribution for the stirred crystallization is bimodal as shown in Figure 1D with every trial producing a high enantiomeric excess as shown in Figure 1C. This bimodal distribution is fundamentally different from that of the unstirred case. It is a direct manifestation of symmetry breaking. The same processes also occur in the crystallization of $NaBrO_3$ (unpublished data).

Chiral symmetry breaking is possible when there is chiral autocatalysis and competition for solute (direct or indirect) between the two enantiomers. Both factors may result from the simple act of stirring. The proposed mechanism involves secondary nucleation and a sensitive dependence of nucleation rate on supersaturation.

(1) Kondepudi, D. K.; Kaufman, R.; Singh, N. *Science* **1990**, *250*, 975-976.
(2) Denk, E. G.; Botsaris, G. D. *J. Cryst. Growth* **1972**, *13/14*, 493.
(3) Kipping, S. T.; Pope, W. J. *Nature* **1898**, *59*, 53.
(4) Hegstrom, R.; Kondepudi, D. K. *Sci. Am.* **1990**, *262*, 108-115.
(5) Bouchiat, M.-A.; Pottier, L. *Science* **1986**, *234*, 1203-1210.
(6) Hegstrom, R. A.; Rein, D. W.; Sandars, P. G. H. *J. Chem. Phys.* **1980**, *73*, 2329-2341.
(7) Mason, S. F.; Tranter, G. E. *Mol. Phys.* **1984**, *53*, 1091-1111.
(8) Tranter, G. E. *Mol. Phys.* **1985**, *56*, 825-838.
(9) Kipping, F. S.; Pope, W. J. *J. Chem. Soc. (London) Trans.* **1898**, *73*, 606-617.
(10) Pincock, R. E.; Perkins, R. R.; Ma, A. S.; Wilson, K. R. *Science* **1971**, *174*, 1081-1020.
(11) *Oscillations and Travelling Waves in Chemical Systems*; Field, R. J., Burger, M., Eds.; Wiley: New York, 1985.

0002-7863/93/1515-10211$04.00/0

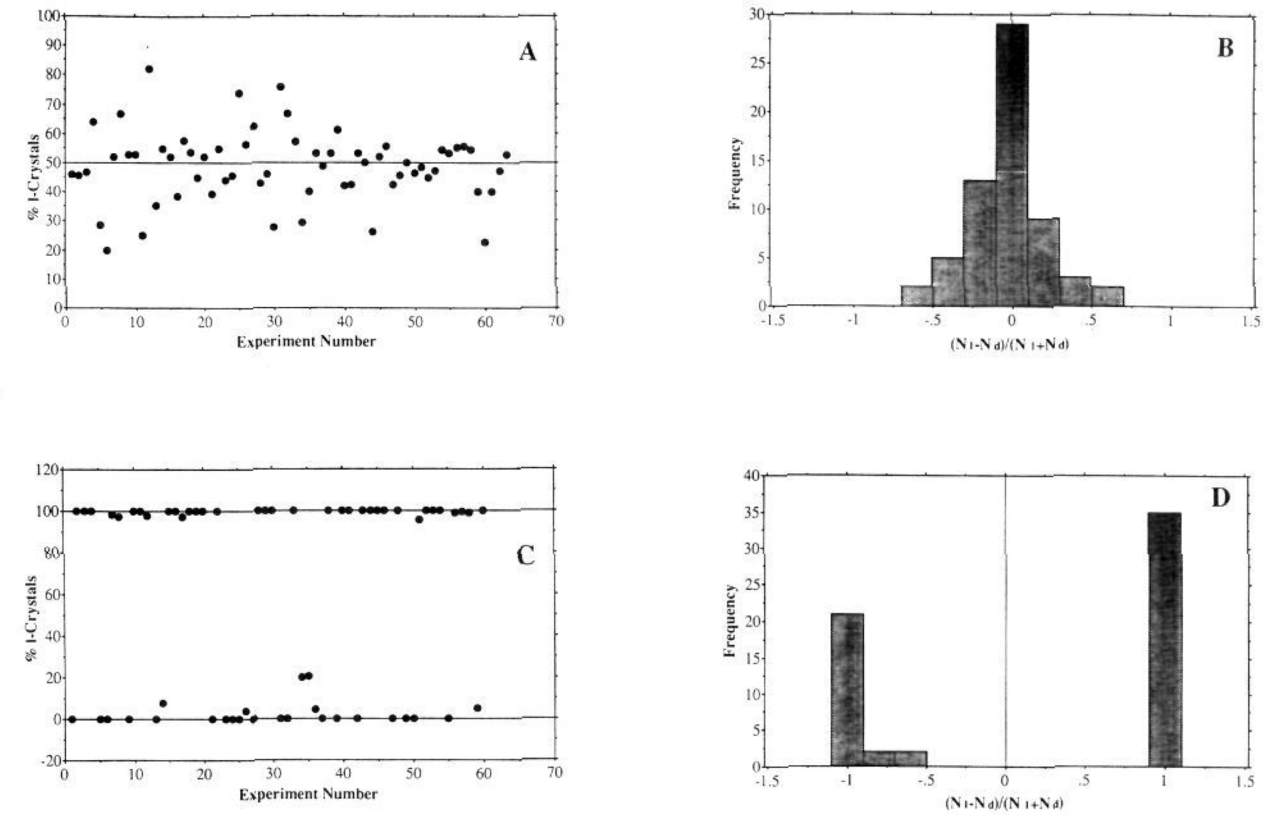

Figure 1. **(A)** Scatter gram showing percent *l*-crystals in a sample of 63 unstirred crystallizations of $NaClO_3$. **(B)** Histogram of crystal enantiomeric excess for the data in part A showing a Gaussian-like monomodal distribution. **(C)** Scatter gram showing percent of *l*-crystals for 60 stirred crystallizations of $NaClO_3$. **(D)** Histogram of the data in part C showing a bimodal distribution.

Secondary nucleation is known to occur in stirred systems.[12–16] This secondary nucleation can cause chiral autocatalysis. In this process, the surface of a crystal in contact with fluid in motion generates new crystal nuclei. The handedness of these secondary crystals is the same as that of the "mother crystal".[2,16] Secondary nucleation can also occur through solid-solid contact (for example, a stirrer coming into contact with the crystal), in which large numbers of secondary crystals are produced but not as a result of macroscopic breakage of the original crystal.[13,15,17]

Chiral autocatalysis should be expected to be a symmetric phenomenon and cannot by itself explain the observed symmetry breaking resulting in a large enantiomeric excess in stirred crystallization. If a primary *l*-crystal can nucleate and multiply through secondary nucleation, then so can a *d*-crystal leading to a chirally symmetric outcome. Proliferation of crystals of a particular handedness must have the effect of suppressing the proliferation of crystals of opposite handedness, hence competition. Such competition can arise as a consequence of sensitive dependence of both primary and secondary nucleation rates and crystal growth rates on supersaturation. As a result of primary nucleation of the "first crystal" and subsequent rapid production of secondary nuclei, the concentration (and hence supersaturation) decreases to a level at which nucleation rates are virtually zero. Stirring increases not only the rate of secondary nucleation but also the rate of growth of nuclei, further contributing to the rate at which the concentration decreases. Once the concentration decreases below the nucleation threshold no new nuclei are created, in particular, nuclei of handedness opposite to that of the "first crystal". In this indirect way the growth of crystals of a particular handedness has the effect of suppressing the growth of the other.

To check the validity of this proposed mechanism experimentally, we followed the concentration of $NaClO_3$ during stirred and unstirred crystallization. According to the proposed mechanism, when crystallization begins, a more rapid decrease in the concentration of solute should occur in the stirred system. We have also developed a computer simulation using stochastic kinetic equations for nucleation and crystal growth. The time variation of concentration predicted by these equations gave us a more detailed understanding of the symmetry breaking process by allowing access to parameters that are difficult to manipulate experimentally.

Experimental Section

The data shown in Figure 1 are for a slow evaporation rate; the evaporation occurred at about 20 °C with a tissue paper covering the beakers. The increase of concentration was rather slow in this case. For this setup the time required for collecting concentration vs time data would be rather long. Hence we performed the same experiment at a higher temperature and faster stirring rates and with uncovered beakers.

Stirred and unstirred solutions close to saturation concentration were placed in 100-mL jacketed beakers to maintain a constant temperature of 45 °C. A 0.5-inch Teflon stir bar was used in the stirred system. The stirring rate was approximately 1000 rpm. Data for the stirred and unstirred systems were collected simultaneously so that the conditions under which the solvent was evaporating were the same for the two systems. As the solvent evaporated, crystals nucleated and grew in both systems. During this process, the concentration of $NaClO_3$ in the solution was monitored through the measurement of refractive index (RI). A

(12) Botsaris, G. D.; Denk, E. G. In *Annual Reviews of Industrial and Engineering Chemistry, 1970*; Weekman, V. W., Ed.; American Chemical Society: Washington, DC, 1972; pp 337–350.
(13) Jancic, S. J.; Grootscholten, P. A. M. *Industrial Crystallization*; D. Reidel Publishing Co.: Boston, 1984.
(14) Strickland-Constable, R. F. In *Crystallization in Solution: Nucleation Phenomenon in a Growing Crystal System*; Estrin, J., Ed.; Am. Inst. Chem. Eng.: New York, 1972; Vol. 68, pp 1–7.
(15) Randolph, A. D.; Larson, M. D. *Theory of Particulate Processes*, 2nd ed.; Academic Press: San Diego, 1988.
(16) Wissing, R.; Elwenspoek, M.; Degens, B. *J. Cryst. Growth* **1986**, *79*, 614–619.
(17) McBride, J. M.; Carter, R. L. *Angew. Chem.* **1991**, *30*, 293–295.
(18) Turnbull, D.; Fisher, J. C. *J. Chem. Phys.* **1949**, *17*, 71.

calibration of the concentration vs RI was found to be linear to a good approximation in the concentration range of interest ($R^2 = 0.942$). Since RI changes with temperature, a temperature vs RI calibration was also performed to make corrections for small variations (less than 1.0 °C) in temperature that may occur during the experiment. Refractive index was measured with an Auto-Abbe refractometer which has the capability to measure refractive index to an accuracy of ±0.00005 and the temperature of the sample to an accuracy of ±0.1 °C. Since crystallization is a relatively slow process, maintaining a constant temperature, though essential, was not difficult.

As the solution evaporated, the concentration increased until crystallization began to occur. Initially the crystals nucleated at the surface. For the stirred and the unstirred solutions the refractive index was monitored for periods ranging from 5 to 10 h. After most of the crystallization had occurred and the concentration has reached a steady value, the crystals were allowed to grow (for several days) until they reached a size large enough to have detectable optical activity. Then the *l*- and *d*-crystals were identified using a pair of polarizers, manually separated and counted.

In addition, to obtain approximate values of the nucleation rates that can be used to set the parameters in the kinetic equations, the unstirred system was observed for many hours with a video camera attached to a frame grabber (on a Mac II). Images captured at regular intervals of time were analyzed for the number of crystals. From these data an approximate nucleation rate was obtained.

Stochastic Kinetic Equations

The proposed kinetic model can be used to formulate a set of differential equations that incorporate the stochastic nature of crystallization. Though the experimentally measured variable is the concentration, it is more convenient to formulate the kinetic equations in terms of amounts of H_2O and aqueous $NaClO_3$.

The processes that drive the crystallization are (i) evaporation (ii) homogeneous and heterogeneous primary nucleation, (iii) stirring-dependent secondary nucleation, and (iv) crystal growth. We define the following variables:

M_w = moles of water in the solution

M_s = moles of solute in the solution

$C = M_s/M_w$, the concentration expressed as a molar ratio (Concentration defined in this way is independent of temperature. Further, evaporation rates of water are more easily measured in terms of the change of mass of water. It is dimensionless and convenient for theoretical formulation of the kinetics.)

C_s = the concentration at saturation (At this stage of the theory, the dependence of C_s on the size of the solute particles is not taken into consideration.)

$E(T)$ = the evaporation rate constant (mol/s/unit area) which is a function of temperature, T

A = area of the solution surface at which the solvent evaporates

N_l = the number of *l*-crystals

N_d = the number of *d*-crystals

ρ = density of the crystal phase (mol/unit volume)

σ_l = the total surface area of the *l*-crystals

σ_d = the total surface area of the *d*-crystals

$P(T,C)$ = stochastic primary nucleation rate which is a function of temperature (T) and concentration (C)

$2H$ = stochastic nucleation rate for nuclei growing at the solution surface

$S(T,C,s)$ = secondary nucleation rate which is a function of temperature (T), concentration (C), and stirring rate (s)

$G(T)$ = crystal growth rate constant as a function of temperature

With the variables thus defined the following kinetic equations are obtained:

$$\frac{dM_w}{dt} = -EA\frac{M_w}{M_w + M_s} \tag{1}$$

$$\sigma_l = \sum_{k=1}^{N_l} 4\pi r_{lk}^2 \qquad \sigma_d = \sum_{k=1}^{N_d} 4\pi r_{dk}^2 \tag{2}$$

Here r_{lk} is the "radius" of the k^{th} *l*-crystal etc.

$$\frac{dM_s}{dt} = -\rho(\sigma_l + \sigma_d)\frac{dr}{dt} = -\rho(\sigma_l + \sigma_d)G(C - C_s) \tag{3}$$

And the linear crystal growth rate is assumed to be:

$$\frac{dr}{dt} = G(C - C_s) \tag{4}$$

$$\frac{dN_l}{dt} = P_l + S_l + H \tag{5}$$

$$\frac{dN_d}{dt} = P_d + S_d + H \tag{6}$$

Under experimental conditions, primary nucleation is mostly due to heterogeneous nucleation, so that homogeneous nucleation may be ignored. For the rate of heterogeneous nucleation, P_l and P_d, we used the following expressions suggested by Randolph:[15]

$$\text{rate} = B\exp\left[\frac{-16\pi N_A\sigma_B v^2}{3(RT)^3[\ln(C/C_s)]^2}\right] \tag{7}$$

In which B is a pre-exponential factor that depends on the number of nucleation sites, N_A = Avogadro's number, v = molar volume of solid $NaClO_3$, σ_B = the surface energy constant that includes factors dependent on nucleation sites, and R is the gas constant. If σ is the surface energy of the crystal nucleus and b is a factor that depends the nucleation site, then $\sigma_B = \sigma^3 b$ (see ref 15, p 116). In the simulation σ_B is taken to be an adjustable parameter. The form of expression 7 is based on the theory of nucleation rates developed by Turnbull and Fisher.[18] Since the stochastic nature of nucleation is important to the processes being studied, we define the nucleation rates P_l and P_d in eqs 5 and 6 as follows.

$P_l = P_d \equiv$ Poisson distributed random function with an average value equal to:

$$B\exp\left[\frac{-16\pi N_A\sigma_B v^2}{3(RT)^3[\ln(C/C_s)]^2}\right] \tag{8}$$

For symmetry breaking processes, the most important feature is the dependence of P_l on the supersaturation ratio C/C_s. The constants in this expression are adjusted to give the experimentally observed nucleation rate. To more fully explain the observed symmetry breaking, we also found that it was necessary to introduce an additional random source of nucleation, H, as might occur on the surface of the solution (several minutes before nucleation begins in the bulk of the solution). This term is included in eqs 5 and 6.

The phenomenon of secondary nucleation has been much studied in the context of industrial crystallization.[13,15] The microscopic nature of this process, however, is still in question.[16] One of the commonly suggested rate laws for secondary nucleation[15,19] is of the form:

$$S_l = s\sigma_l K_s(C - C_s)^\alpha \tag{9}$$

in which s is the stirring rate, K_s is a constant that may depend on the temperature, and σ_x is the total surface area of the crystals of type x (x being *l* or *d*). Reported values of the exponent α range from 0.5 to 2.5[19] for various compounds.

The nature of the observed random outcomes of the experiments necessitates formulation of these equations as stochastic differ-

(19) Garside, J. *Chem. Eng. Sci.* **1985**, *40*, 3–26.

ential equations in which P_l and P_d are random functions. This is an essential feature of this process that cannot be ignored; as was noted by McBride and Carter,[17] even though a large number of crystals are involved, statistical aspects of the initial nucleation are a determining factor for the final outcome. N_l and N_d then become stochastic variables that are properly described through a probability distribution.

Equations 1–9 are the kinetic equations of the system. If the suggested mechanism is a good approximation, then it must be able to produce the experimentally observed time variation of concentration and the statistical aspects of N_l and N_d. It does not seem possible to obtain analytical solutions for the time variation of the concentration, $C(t)$, and the probability distribution of N_l and N_d for the above set of nonlinear coupled stochastic differential equations. Hence we sought numerical solutions to these equations by developing an appropriate computer simulation code. The computer code was written in Mathematica, because of the convenience of integrated features it offers.

Computer Algorithm for Numerical Solutions

To have a quantitative understanding of the kinetics, a computer code to simulate the kinetics described by eqs 1–9 was developed using Mathematica. The main structure of the code is as follows:

(a) The mass of water was decreased according to the specified evaporation rate and the concentration updated.

(b) When the concentration exceeds saturation, primary l- and d-nuclei are generated with equal probabilities in accordance with eq 8 using a random number generator. The time of generation of each nucleus is recorded. Mathematica has the capability of generating random numbers with most of the common distributions. To simulate the formation of nuclei at the surface, seed crystals are randomly introduced into the system when the concentration exceeds saturation. (As will be discussed below, this feature was necessary to obtain the observed symmetry breaking.)

(c) After nucleation, each crystal is made to grow at a concentration dependent rate given by eq 4. As the crystals grow, the solute deposited on the crystals is computed assuming an average spherical geometry. The corresponding amount of solute is removed from the solution and the concentration is updated.

(d) As the crystals grow, the process of secondary nucleation comes into effect. In the simulation it was found that the symmetry was broken only when a *minimum size* for the production of secondary nuclei was introduced. Thus when the crystals reach the specified minimum size, secondary nuclei are generated at a rate specified by eq 9. As with the primary nuclei, the growth of the secondary nuclei is taken into account and the concentration updated.

Thus the code not only generates the concentration vs time data but also gives the total number of primary and secondary l- and d-crystals created and their size (radii).

Results and Discussion

The experimentally obtained variation of concentration with time for the stirred and the unstirred systems, for $T = 45$ °C, is shown in Figure 2. In every case of the stirred crystallization large asymmetry was produced. Typical data for four stirred and one unstirred crystallizations are shown in Table I.

For the stirred solution, the effects of secondary nucleation and the resulting rapid drop in concentration can clearly be seen. In contrast, the concentration varies much more slowly in the unstirred system and reaches a higher value. The small but noticeable difference in the initial linear growth of concentration is due to the slightly larger evaporation rate in the stirred system. This is because the vortex generated by the stirring enlarges the area of liquid surface resulting in a larger evaporation rate for the stirred system. In addition, due to the cooling caused by evaporation, the surface temperature can also be expected to be

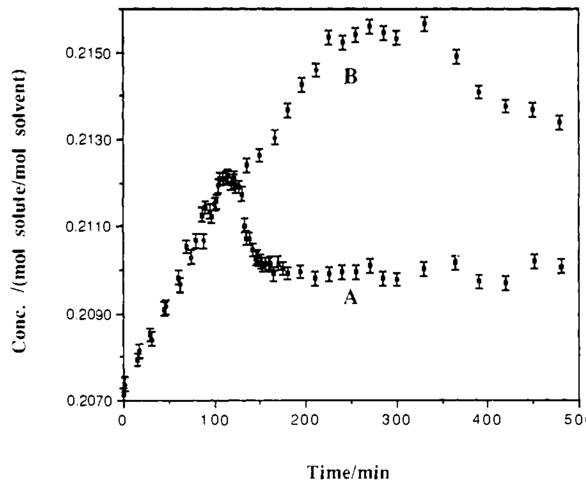

Figure 2. Typical concentration vs time curves for stirred (A) and unstirred (B) crystallization of $NaClO_3$. The sharp drop in the concentration for the stirred solution is due to secondary nucleation. The number of l- and d-crystals generated in these runs is given in Table I, samples 3 and 5.

Table I. Data from Crystallizations, Four Stirred and One Unstirred, When the Evaporation Occurred at 45 °C[a]

sample no.	N_l	N_d	mass of l-crystals in g	mass of d-crystals in g
1 (stirred)	3	608	0.035	7.681
2 (stirred)	6	594	0.031	6.094
3 (stirred)[b]	411	22	6.951	0.428
4 (stirred)	2	1751	0.061	13.534
5 (unstirred)[b]	195	210	5.769	5.126

[a] Stirring was done with a 0.5-in. Teflon stirrer at about 1000 rpm. [b] Concentration vs time plots for samples 3 and 5 are shown in Figure 2.

lower than the bulk temperature for the unstirred system but not so for the stirred system, because stirring eliminates temperature gradients. This difference also contributes to the lowering of the evaporation rate of the unstirred system. Quantitative fit using the computer simulation of the processes gives an evaporation rate of 1.38×10^{-5} and 1.1×10^{-5} mol of H_2O/s for the stirred and unstirred systems, respectively.

A comparison between the concentration obtained by the kinetic eqs 1–9 and the experimental data for the stirred crystallization is shown in Figure 3. Though there are several parameters in the kinetic equations, many of these parameters are restricted in their range by the experimental data. Thus, the evaporation rate constant $E(T)$ is fixed by the initial linear part of the concentration curve. The rate of nucleation, obtained by video observations, was found to be in the range of 1–2 nuclei per minute for the entire system. (Both in the stirred and unstirred cases, some of the crystals nucleate at the solution surface.) Accordingly, the parameters B and σ_B in eq 7 are adjusted such that, in the experimental range of the saturation ratio (C/C_s), the nucleation rate is 0.2 nuclei/min when $(C/C_s) = 1.001$ and reaches a value of 2 nuclei/min when $(C/C_s) = 1.04$. For these conditions $B = \exp[-3.34]$ and $\sigma_B = 2.06 \times 10^{-24}$ (J/cm^2)^3. An approximate value for growth rate constant G and E can be obtained from experimentally measured values. In the simulation we set $G = 13.1 \times 10^{-3}$ cm/s/(unit excess concentration) and $E = 1.38 \times 10^{-5}$ mol of H_2O/s for the stirred system. The most uncertain parameters are those that are in the secondary nucleation rate. In the stirred system, the maximum value of the concentration depends on these parameters. The values that produce the experimentally observed concentration variations shown in Figure 3 are the following: $K = 5.0 \times 10^8$, $s = 2$, $\alpha = 2.75$. The values of the product (Ks) and the exponent α determine the total number of crystals produced in each run. The particular values specified above produced about 10^4 crystals.

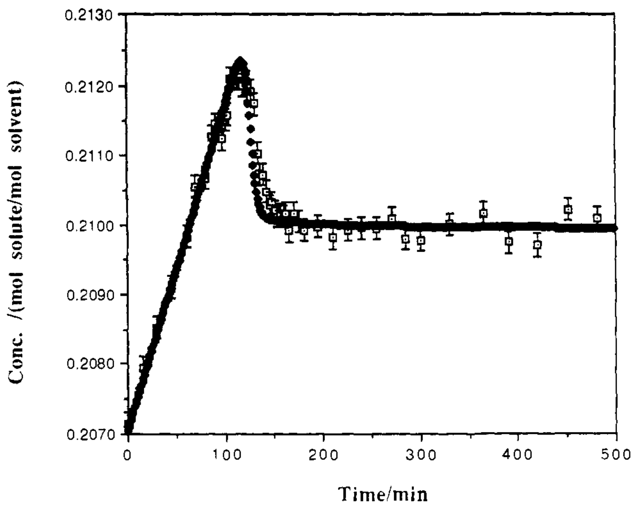

Figure 3. Comparison of the concentration vs time curves predicted by eqs 1–9 and the experimental data for stirred crystallization. The values of the parameters used in the equations are the following: $C_s = 0.2099$; $E = 1.38 \times 10^{-5}$ mol/s; $G = 13.13 \times 10^{-3}$ cm/s/(unit concentration); $B = \exp[-3.4]$; $\sigma_B = 2.06 \times 10^{-24}$ (J/cm^2)^3; $\nu = 45.24$ mL/mol; $K = 5.0 \times 10^8$; $s = 2$; $\alpha = 2.75$; $R_{min} = 0.09$ cm; $R_s = 0.05$ cm.

Computer simulation of the crystal kinetics reveals many important and remarkable aspects of the processes of chiral symmetry breaking. For example, if the evaporation rate and the primary nucleation rate are fixed, then the conditions under which symmetry will be broken can be determined. In the simulation, we found that symmetry is broken only when we introduced a minimum crystal size for the production of secondary nucleation. In the production of secondary nuclei hydrodynamic shear, crystal–stirrer collision and crystal–crystal collisions are involved; the minimum size for noticeable secondary nucleation may be involved in some or all of these processes. A more direct observation of such a minimum seed size for secondary nucleation was reported for the crystallization of potassium alum.[20] Otherwise, the primary nucleation rate of about 1–2 per min was too rapid, and before the concentration dropped due to secondary nucleation from one crystal, several other crystals were produced. If all of these crystals were assumed to produce secondary nuclei, the resulting enantiomeric excess was found to be small. Also, the exponent α had to be sufficiently large so that the rate of secondary nucleation was significant only in a very small range of supersaturation. This restriction on α allows all the secondary nucleation to arise from only one crystal. As was noted by McBride and Carter,[17] it is remarkable that one crystal can so dominate the entire system, not simply in principle or through an occasional chance, but virtually in every stirred crystallization. The required sequence of events is as follows: a crystal randomly nucleates at some time and begins to grow (typically at the solution surface). As the supersaturation increases, more crystals are produced at an increasing rate, a fact observed in the experiments. When the first crystal reaches a critical size, if the supersaturation is high enough, it begins to produce secondary nuclei at an appropriately fast rate. This rapid production of secondary nucleation can be due to hydrodynamic shear or due to collision with the stirrer. This causes the concentration to drop slowing the growth of other crystals already produced and the rate of production of new nuclei. This drop in concentration should occur such that, before any other crystal reaches a size at which it can produce secondary nuclei, the concentration drops to a value at which the rate of secondary nucleation for all the crystals in the system is virtually zero.

The above subtle requirement of this small "window of secondary nucleation" can be seen through computer simulation. This is illustrated in Figure 4. Curve A shows the variation of concentration with the generation of a d-crystal at $t = 55$ min of size 0.05 cm. The minimum size for the secondary nucleation was taken to be 0.09 cm. These parameters lead to the breaking of symmetry: $N_l = 67$ crystals and $N_d = 8524$ crystals. Keeping all the parameters exactly the same and changing the size of the initial crystal to 0.02 cm, the system produced a much lower crystal enantiomeric excess: $N_l = 8541$ crystals and $N_d = 18818$ crystals. The corresponding time variation of concentration is shown in curve B. In the former case the "window of secondary nucleation" is much smaller than that of the later.

(20) Kubota, N.; Fuliwara, M. *J. Chem. Eng. Jpn.* **1990**, *23*, 691–696.

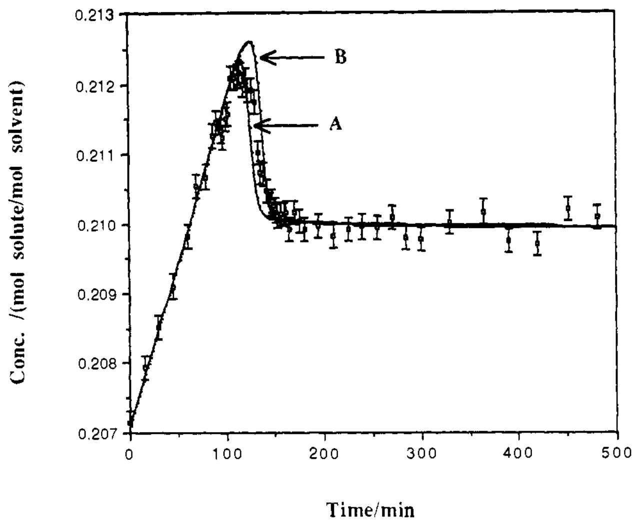

Figure 4. The effects of seed size on the concentration vs time curve as predicted by the kinetic eqs 1–9. Curve A shows the results of a d-seed of size 0.05 cm introduced at time $t = 55$ min. Curve B shows the results for a d-seed of size 0.02 cm also introduced at $t = 55$ min. In both cases the minimum radius for secondary nucleation was set at 0.09 cm. The case corresponding to curve A produced 67 l-crystals and 8524 d-crystals while the case corresponding to curve B produced 8541 l-crystals and 18818 d-crystals. It was not possible to produce experimentally observed crystal enantiomeric excess if a minimum size for secondary nucleation was not introduced.

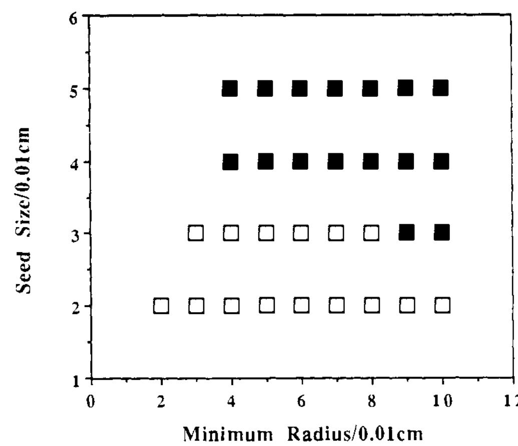

Figure 5. Regions in the parameter space of seed size, R_s, and minimum radius for secondary nucleation, R_{min}, in which N_d was greater than 90% are indicated by the dark squares. All other parameters are the same as in Figure 3. Simulations in which N_d was found to be less than 90% are shown by the light squares. If R_s is greater than R_{min}, symmetry breaking will occur and N_d will be larger than 90%. One such point ($R_s = 5$, $R_{min} = 4$) is included among the dark squares.

In the experiments, however, symmetry was consistently broken. This means that there is a range for the seed size that can produce symmetry breaking. Let the seed size be denoted by R_s and the minimum size for secondary nucleation by R_{min}. Since the value of R_{min} is not known, we explored the parameter space of R_s and

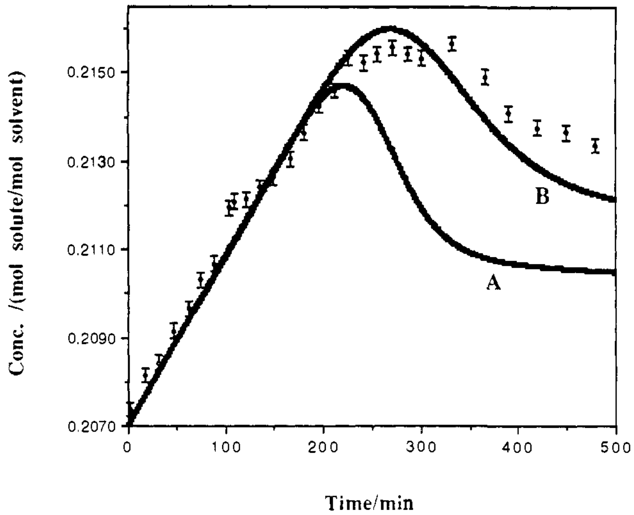

Figure 6. Comparison of the concentration vs time curves predicted by eqs 1–9 and the experimental data for unstirred crystallization. The values of the parameters used in the equations for curve A are the following: $C_s = 0.2099$; $E = 1.11 \times 10^{-5}$ mol/s; $G = 2.95 \times 10^{-3}$ cm/s/(unit concentration); $B = \exp[-3.4]$; $\sigma_B = 2.06 \times 10^{-24}$ (J/cm^2)^3; ν = 45.24 mL/mol. Curve B shows the results of the simulation if finite-volume effects are included in the kinetics.

R_{min} to determine the region in which symmetry is broken. R_s was varied from 0.01 to 0.05 cm and R_{min} was varied from 0.01 to 0.1 cm. Figure 5 shows the cases in which the percent of d-crystals was greater than 90 for a d-seed. This showed that if at time t = 55 min there is no crystal of size greater than 0.02 cm, the number of d-crystals, N_d, will be less than 90%; if by this time R_s is 0.03 cm or larger N_d will be larger than 90%. Though a range of R_{min} resulted in a N_d larger than 90%, a good fit for the experimentally observed time variation of the concentration could be obtained only when R_{min} was greater than 0.07 cm. The above observations show that in symmetry breaking observed in stirred crystallization, a minimum size for secondary nucleation is clearly involved. This minimum size could be a consequence of the shear forces experienced by the crystal surface for given stirring conditions. The relative velocity between the crystal and the solution will be higher for a larger crystal resulting in a larger shear force. These speculations will be investigated in future experiments.

The computer code could also simulate unstirred crystallization. A comparison of the experimental data and simulation results is shown in Figure 6. Curve A shows the results of simulation in which the evaporation rate is adjusted to fit the experimental data ($E = 1.1 \times 10^{-5}$ mol of H_2O /s). The other parameters were $G = 2.95 \times 10^{-3}$ cm/s/(unit excess concentration) and $s = 0$. All other parameters are the same as those used for the stirred crystallization. As can be seen, the experimentally observed rise and drop in concentration is much slower than that produced by the simulation. The main reason for this discrepancy is that in the simulation each crystal grows independently, uninfluenced by the growth of other crystals. In the experiment, however, due to space limitation the growth of a crystal is slowed by the presence of other crystals in its neighborhood. Further, after sufficient numbers of crystals are produced, new nuclei produced do not grow as independent crystals but are incorporated into the existing crystals. Thus, in reality both the rate of production of new crystals and the growth rates decrease with time. As a first approximation, we included these effects in the simulation code by altering the nucleation rate by the factor $[1 - (N_{total}(t)/N_{max})]$ in which $N_{total}(t)$ is the total number of crystals at time t and N_{max} is a fixed parameter that corresponds to the maximum number of crystals that can be produced in each run. The growth rate was augmented by the decreasing function $\exp[-\beta M_t/M_{s0}]$, in which β is a parameter, M_t is the amount of solute in the solid phase, and M_{s0} is the total amount of solute in the solution. Curve B shows the results of simulation for $N_{max} = 200$ and $\beta = 7$. Though the particular form of the functions used to augment the nucleation and growth rates are arbitrary, we do see that self-limiting growth of crystals is needed to fully understand the time variation of concentration. In the stirred system, since a decrease in the concentration is due to a large number of small crystals that are distributed throughout the entire volume (not just the bottom of the beaker as in the case of the unstirred crystallization), the limitation in growth does not seem to be a major factor needed to obtain the experimentally observed time variation of concentration.

While the present theory explains many of the major experimental observations, the limitations of the theory and computer simulation must be noted. First, the theory does not explicitly take inhomogeneities into consideration. Thus, temperature, concentration, and number of crystals per unit volume are all assumed to be homogeneous. Nucleation and crystal growth do depend on inhomogeneities in these variables. Also, the solubility of a crystal depends on its size; hence, strictly speaking, the concentration at saturation, C_s, depends on the crystal size. A related aspect that has also not been included in the theory is the process of crystal ripening (by which larger crystals grow at the expense of smaller crystals). Crystal ripening must be taken into consideration to theoretically obtain the crystal size distribution. We intend to include these factors in the future developments of the theory and the computer code.

Acknowledgment is made to the donors of The Petroleum Research Fund, administered by the American Chemical Society, for support of this research. We also acknowledge support from NSF-REU for Kim Bullock's participation in this research project. Support was also provided by REACREAC of Wake Forest University. We are grateful to Dr. Wilson Sommerville for his valuable editorial assistance.